

## THE LONG-PERIOD VARIABLE STARS OF M33

JEREMY MOULD, JAMES R. GRAHAM, KEITH MATTHEWS, AND GERRY NEUGEBAUER

Palomar Observatory, California Institute of Technology

AND

JONATHAN ELIAS

Palomar Observatory; and Cerro Tololo Inter-American Observatory

Received 1989 May 22; accepted 1989 July 31

### ABSTRACT

Infrared photometry of long-period variables (LPVs) in M33 shows that the majority of those identified up to now are supergiants. The period-luminosity relation for these stars yields a distance to M33 of 760 kpc with a 10% uncertainty. This uncertainty primarily reflects the uncertain distance of the Large Magellanic Cloud, although the broader  $P-L$  relation of M33 is a contributing factor. Cepheid period-luminosity relations yield a distance at the low end of this range; RR Lyrae stars tend toward the high end. The remaining LPVs are asymptotic giant branch stars. There is one confirmed carbon star among them.

*Subject headings:* galaxies: individual (M33) — stars: long-period variables — stars: pulsation

### I. INTRODUCTION

Over the interval 1982 to 1985 a survey for long-period variables (LPVs) was carried out in M33 using the prime focus camera of the Mayall 4 m telescope at Kitt Peak. Analysis was carried out at Mount Stromlo Observatory, and the first findings were published by Kinman, Mould, and Wood (1987, hereafter KMW). From 1985 to 1988 we carried out a program of infrared photometry of these LPVs at Palomar Observatory, and we present the results here.

### II. VARIABILITY

Observations of a significant number of the KMW program stars were made in 1986 November, 1987 July, and 1988 October. All of them have been observed at least once, and most of them have been measured twice. A handful of stars were observed in 1982 November based on the earlier survey by van den Bergh, Herbst, and Kowal (1975). Until 1988 we used a single channel InSb infrared photometer with a diaphragm of 5"–8" in diameter to make these measurements. In 1988 we used an infrared camera containing a  $62 \times 58$  InSb array. Both instruments were mounted at the  $f/70$  Cassegrain focus of the 5 m Hale telescope, giving a field size for the camera of 18". All observations were calibrated by measurements of CIT/CTIO standard stars (Elias *et al.* 1981). Reduction of the camera frames is outlined by Mould *et al.* (1989). All observations, which were carried out under photometric conditions, are recorded in Table 1.

Since photometry from infrared images is a relatively new procedure, it is worth recording a few details here. Photometry of the camera frames, which were obtained in optical seeing better than 1" FWHM, was carried out inside 2.5 diameter circular areas with the aid of a small correction to total flux (typically 0.04 mag). These aperture corrections were evaluated on relatively bright stars. The linearity correction (Mould *et al.* 1989) was of the same order as the aperture correction, both for standards and program stars. The mean difference between the  $\langle K \rangle$  magnitudes obtained single-channel by Mould (1987), and the camera  $K$  magnitudes for stars with  $K < 15$  mag was  $0.02 \pm 0.03$  mag.

Photometric calibration (Mould 1987) of the photographic data of KMW indicates a mean red amplitude of 0.6 mag. (Amplitude here and below refers to half  $R_{\max} - R_{\min}$ .) In the infrared, however, the amplitude of these variables is much smaller. Variability is nevertheless evident, given that 80% of the  $K$  measurements in Table 1 have an uncertainty less than or equal to 0.03 mag, and more than 93% have errors less than 0.1 mag. Sparse sampling of the light curves of the variables means that we can only give a statistical estimate of the true variation, however. Figure 1 indicates the amplitude of variation at  $K$ . For each multiply observed star  $\delta K = K_i - \langle K_i \rangle$  is plotted versus  $\delta \cos(\phi) = \cos(\phi_i) - \langle \cos(\phi_i) \rangle$ , where  $\phi_i$  is the phase of an individual observation  $K_i$ , and  $\langle K_i \rangle$  is the mean over all  $i$ . In such a plot a set of cosine light curve variables would yield a correlation whose slope is equal to the negative of the mean amplitude. Figure 1 shows a weak correlation ( $r = -0.18$ ) with a slope of  $-0.02 \pm 0.01$ . We conclude that the mean amplitude of the correlated variation at  $K$  in this sample is less than 0.05 mag. By *correlated* variation we mean the amplitude of the variation in phase with the optical light curve. The uncorrelated rms variation in  $K$  is 0.06 mag.

Figure 2 shows that the  $K$  amplitude of this sample of M33 LPVs is less than that of two comparable samples of variable stars, and also examines the correlation of the variation at  $K$  with  $J - K$ . In a sample of LMC LPVs Wood, Bessell, and Fox (1983, hereafter WBF) see an amplitude  $\delta K \leq 0.25$  mag for supergiants and  $\delta K = 0.5$ –1.0 mag for AGB stars. Amplitudes in M33 are smaller both among the brighter and fainter LPVs. There is rather little correlation of  $\delta K$  with  $\delta(J - K)$  (calculated with respect to the mean for each of their multiply observed stars) in the LMC sample. In a third sample, long-period Galactic LPVs ( $P > 500$  days) from Catchpole *et al.* (1982), one sees a similar amplitude to that of the LMC, but perhaps more of a hint of a correlation of redder colors with fainter magnitudes. A correlation in the opposite sense is apparent in the M33 data, but does not seem significant in the light of the photometric uncertainties affecting the fainter stars.

According to the study of LMC M supergiants by Elias, Frogel, and Humphreys (1985), one might expect from the observed  $R$  amplitude in the M33 sample a correlated  $K$

TABLE 1  
INFRARED PHOTOMETRY OF LPVs IN M33

J.D. <sup>1</sup>	J	H	K	J.D. <sup>1</sup>	J	H	K	J.D. <sup>1</sup>	J	H	K <sup>2</sup>
P1322				P22330				Q17032			
6747.5	16.90	15.95	15.48	6983.5	15.21	14.30	13.81	6748.5	15.22	14.48	14.25
6984.5	16.65(4)	15.82	15.54(4)	7460.5	15.14	14.21	13.75	7460.5	15.12	14.35	14.10
7459.5	16.69(6)	15.81	15.61	P23152				Q17068			
P2426				6747.5	17.76(8)	16.82(5)	16.15(6)	6747.5	17.96(10)	16.96(6)	16.64(12)
6747.5	14.72	14.00	13.67	6988.5	17.73(9)	16.84(6)	15.83(7)	7460.5	18.28(6)	17.06(4)	16.53(13)
5274.5	14.94	14.18	13.81	7460.5	17.35(10)		16.00(5)	Q17675			
P3482				P23182				6748.5	14.81	14.08	13.76
6748.5	15.43(9)	14.81(6)	14.53(5)	6747.5	15.08	14.31	14.04	7459.5	14.89	14.05	13.72
5274.5	15.53	14.83	14.57	7459.5	15.04	14.23	13.90	Q18180			
6984.5	15.52	14.83	14.57(5)	P23324				6748.5	15.80	15.05	14.73
P5900				6748.5			15.25	6983.5	15.81	15.09	14.67(6)
6748.5			16.4(6)	7459.5	16.07	15.24	15.12	7459.5	15.88	14.99	14.81
7459.5	18.19(15)	16.79(17)	15.97(16)	P24355				Q18569			
7460.5	17.84(4)	16.64(7)	16.3(15)	6747.5	14.92	14.15	13.78	6748.5	16.21	15.37	15.07
P6283				7460.5	14.92	14.10	13.74	6982.5	16.23	15.27	14.95
6748.5	14.11	13.50	13.24	P25017				Q21308			
7459.5	14.27	13.59	13.37	6748.5	14.51	13.76	13.41	6747.5	15.02	14.35	14.16
P6836				7459.5	14.58	13.81	13.51	7460.5	15.16	14.46	14.21
6748.5	14.98	14.24	13.92	P28639				Q21736			
7460.5	15.03	14.15	13.89	6747.5	14.98	14.18	13.79	6748.5	15.70	15.00	14.66
P7022				7459.5	14.94	14.09	13.75	7459.5	15.74	14.88	14.61
6747.5	16.59	15.81	15.49	P28986				Q21740			
7460.5	16.63(4)	15.64	15.46	6748.5	14.71	14.00	13.68	6748.5	14.68	13.85	13.53
P9441				P29476				5274.5	14.52	13.74	13.40
6748.5			15.91(6)	6983.5	14.94	14.24	13.88	Q21765			
6986.5	17.66(9)	16.53(4)	16.03(7)	7460.5	15.17	14.32	13.96	7460.5	15.86	15.03	14.72
P11172				P29926				Q22366			
6747.5	15.27	14.37	13.91	7460.5	14.45	13.70	13.41	6748.5	14.88	14.30	13.99
7459.5	15.49	14.48	14.07	P32117				6982.5	14.93	14.31	14.05
P11629				6983.5	17.53(14)	16.78(6)	16.06(12)	Q24798			
6748.5			14.87(4)	7460.5	17.69(7)	16.63	16.00	6747.5	15.71	15.01	14.79
7459.5	15.90	15.11	14.88	P32202				6983.5	15.64	14.98	14.77(6)
7460.5	15.85	15.11	14.80	6747.5	15.40	14.60	14.26	Q29211			
P11988				6983.5	15.32	14.59	14.27(4)	6748.5			14.16
6748.5	15.89	15.33	15.10	Q6508				6982.5	15.53	14.65	14.29
7459.5	15.90	15.22	14.84	6747.5	14.89	14.15	13.79	Q29250			
P14476				5274.5	14.84	14.15	13.87	6748.5			15.33(4)
6747.5	15.50	14.74	14.28	7460.5	14.73	13.97	13.77	6983.5	16.21(10)	15.68(6)	15.32(8)
6988.5	15.70	14.94	14.36(4)	Q6512				Q29334			
P16071				6748.5	15.48	14.69	14.53	6748.5	14.96	14.16	13.65
7460.5	15.00	14.22	13.85	6988.5	15.48	14.84	14.65(4)	7459.5	15.08	14.16	13.66
P16339				Q12254				Q29631			
7460.5	14.75	13.97	13.62	6748.5	14.73	13.93	13.50	6747.5	15.54	14.73	14.37
P18694				5274.5	14.71	13.96	13.54	6982.5	15.62	14.85	14.45
6748.5	14.60	13.96	13.39	Q14906				Q31100			
6984.5	14.80	14.11	13.49	6747.5	15.15	14.36	14.08	6748.5	14.57	13.84	13.56
P19844				6983.5	15.20	14.42	14.18	5274.5	14.53	13.78	13.45
6748.5	15.67	15.03	14.58	Q15476				Q31267			
7459.5	15.41	14.74	14.41	6748.5			16.60(16)	6747.5	14.81	14.07	13.86
P20917				7459.5	17.52	16.73(7)	16.73(15)	6983.5	14.72(4)	14.03	13.78
7460.5	14.72	13.97	13.60	Q16350							
P21091				6747.5	14.56	13.88	13.56				
6747.5	14.74	13.96	13.56	7459.5	14.75	14.01	13.74				
6986.5	14.93	14.21	13.77								

NOTES.—Julian date —2,440,000 days. Parentheses enclose photometric uncertainties in hundredths of a magnitude.

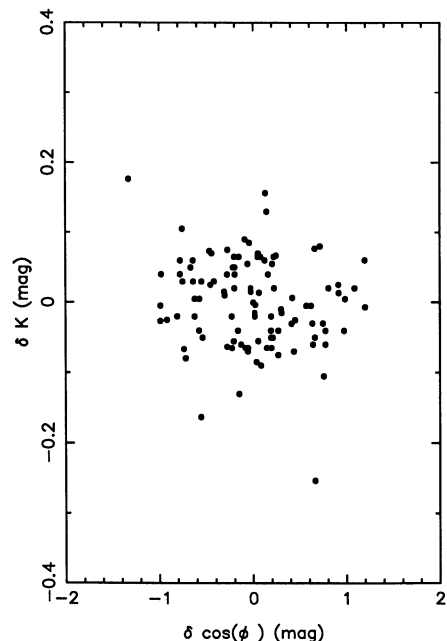


FIG. 1.—An indication of the amplitude of variability of the sample at 2.2  $\mu\text{m}$ . Deviation from the mean  $K$  magnitude is plotted against offset from the mean phase.

amplitude exceeding 0.1 mag. In their simultaneous optical-IR study of the LMC they also found  $\delta(J-K)/\delta K = +0.12 \pm 0.07$ . Although one might attribute the small correlated amplitude of the M33 sample to the well known phase irregularity of LPVs (and there is a separation of a few periods between the infrared and optical photometry in M33), it appears that the uncorrelated variation of the M33 sample is also smaller than that of comparison samples from the Galaxy and the Magellanic Clouds. Small amplitude is thus a real property of the sample; whether this a real property of late-type stars in M33, or a selection effect, it is impossible at present to say.

### III. THE TWO-COLOR DIAGRAM

Figure 3 indicates the location of the program stars in the  $J-H$ ,  $H-K$  diagram. The plotted quantities are  $\langle J \rangle$ ,  $\langle H \rangle$ ,  $\langle K \rangle$ , and we shall refer to  $\langle J \rangle - \langle H \rangle$  as  $J-H$  for simplicity below. (A plot of  $\langle J-H \rangle$  vs.  $\langle H-K \rangle$  is very similar to Fig. 3 because of the small amplitude of variation.) One sigma errors in estimating these quantities are shown explicitly where the combined error exceeds 0.2 mag. The mean errors for the sample are indicated in the lower right-hand corner of Figure 3. Superposed on Figure 3 is the “Mira coffin,” transformed from the SAAO system following Bessell and Brett (1988). The “coffin” contains the intrinsic colors of most M-type Galactic Miras according to Feast *et al.* (1982), and stars outside it with  $H-K > 0.6$  mag are likely to be carbon stars (Reid, Glass, and Catchpole 1988). We conclude that on the whole our sample is only lightly reddened (see also Elias, Frogel, and Humphreys 1985).

Figure 4 is a spectrum of the reddest star in  $H-K$  (P23152), which is a carbon star. The spectrum was obtained in an exposure of 20 minutes with the 5 m telescope, and has a resolution of  $\approx 18 \text{ \AA}$ . The (0, 0) bandhead of the  $\text{C}_2$  Swan system is clearly visible at  $\approx 5600 \text{ \AA}$ . The spectrum is similar to spectra of Magellanic Cloud carbon stars published by Mould and

Aaronson (1980). Other stars which fall outside the “coffin” on the red side are P5900, P9441, P32117, and Q17068, but spectra are unavailable at this time. We shall see that these five stars have a well defined mean bolometric magnitude consistent with that of carbon stars in the Magellanic Clouds. Two stars are much bluer in  $H-K$  than the rest of the sample, P23324 and Q15476. With the exception of P32117 all of the above mentioned stars are relatively short-period variables.

### IV. THE H-R DIAGRAM

We begin with a color-magnitude diagram, Figure 5, showing  $K$  versus  $J-K$ . Horizontal error bars are only indicated where the relevant value exceeds 0.15 mag. The mean

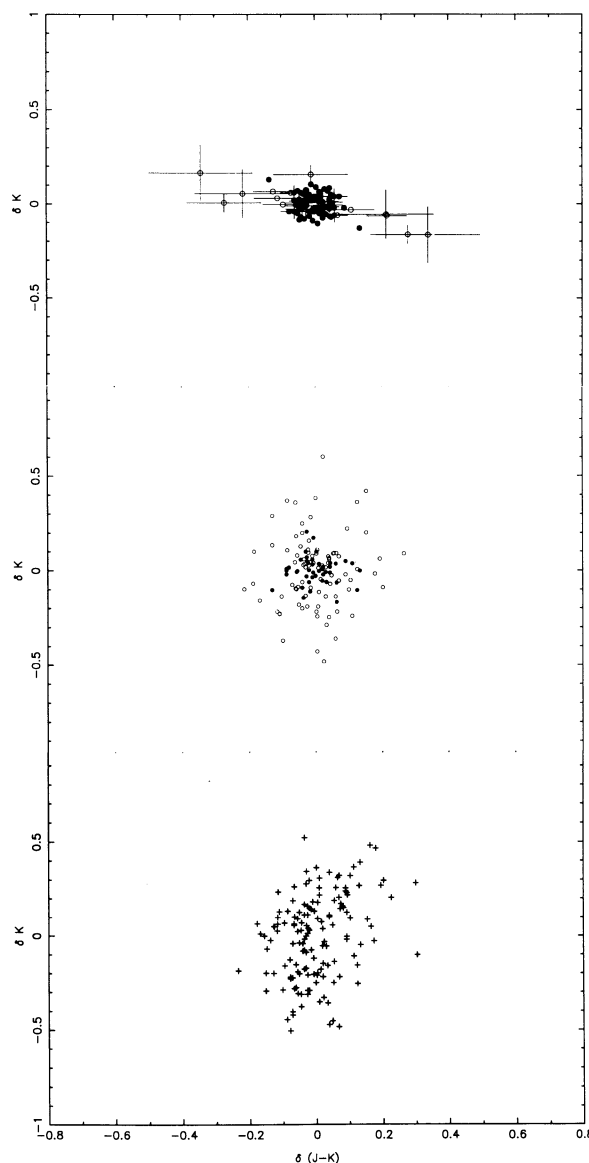


FIG. 2.—Deviation from the mean  $K$  magnitude is plotted against deviation from the mean  $J-K$  color for three samples. The top sample is the present sample of M33 LPVs. Stars with  $K > 15$  mag are shown as open circles; stars with  $K < 15$  mag are shown as filled circles. The central sample is that of Wood, Bessell, and Fox (1983). LMC stars with  $K > 8.5$  mag are shown as open circles; stars with  $K < 8.5$  mag are shown as filled circles. The bottom sample consists of Galactic LPVs with  $P > 500$  days observed by Catchpole *et al.* (1979).

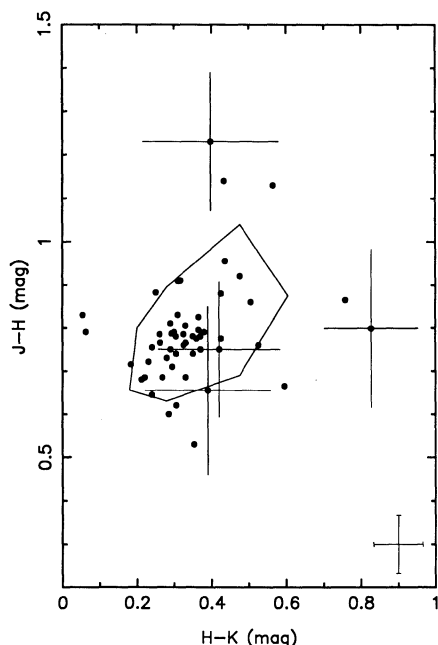


FIG. 3.—The infrared two-color diagram. The rms error in establishing  $\langle J \rangle$  etc. is shown in the lower right-hand corner. Only the largest individual error bars are plotted. The superposed polygon is called the “Mira coffin,” and contains dereddened Galactic Miras of spectral type M.

error in  $J-K$  is indicated at the top right of the figure. The most striking feature of Figure 5 is the segregation of the five carbon star candidates (§ III) in the right-hand corner of the color-magnitude diagram. (Note that two symbols are almost superposed at  $J-K = 1.63$  and  $K \approx 16$  mag.) Supposing that these stars are in fact all carbon stars, we can understand this segregation if there is an upper limit to the luminosity of AGB carbon stars in M33, just as there is in the Magellanic Clouds (Cohen *et al.* 1981).

To estimate the luminosity of LPVs, we adopt the bolometric corrections calculated by Frogel, Persson, and Cohen (1980) and a uniform reddening of stars in M33 of  $A_V = 0.3$  mag (Feast 1988). Apparent bolometric magnitudes are recorded in Table 2, supposing that all the program stars are M stars,

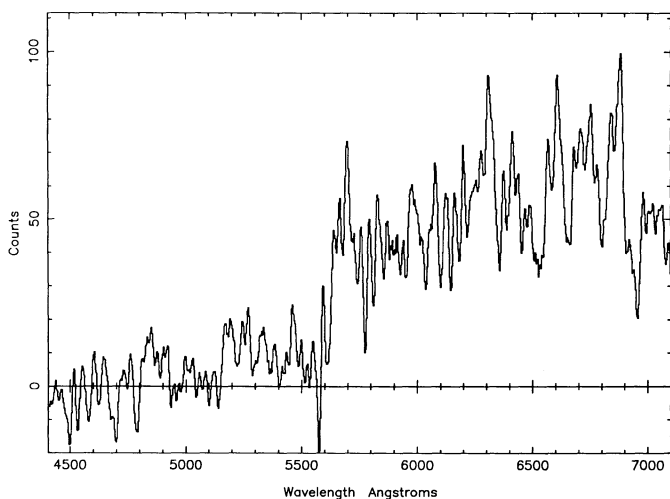


FIG. 4.—Spectrum of P23152, a carbon star

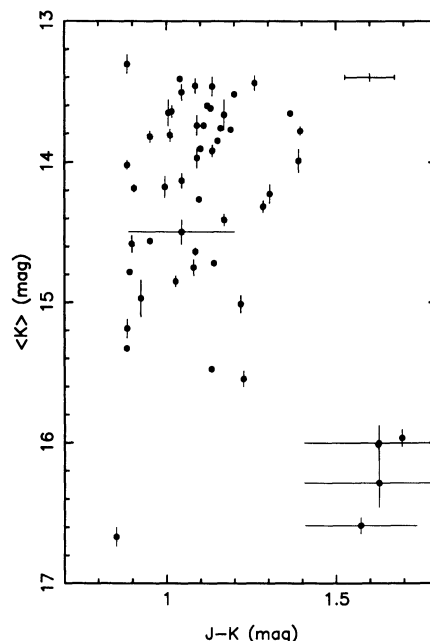


FIG. 5.—An H-R diagram formed from  $\langle K \rangle$  vs.  $\langle J \rangle - \langle K \rangle$  in Table 2

except P5900, P9441, P23152, P32117, and Q17068. The absolute bolometric magnitude of the three brightest of the above is  $-5.4$  mag, if we adopt Mould's (1988) distance modulus of 24.5 for M33. If the LMC is 6.2 mag closer than M33 (Mould 1988), the brightest<sup>1</sup> carbon stars in the LMC have  $M_{\text{bol}} \approx -5.6$  mag (Cohen *et al.* 1981).

The maximum luminosity of the M type LPVs in Figure 5 is also well defined, and more likely to refer to a complete sample. Star P6283 has  $M_{\text{bol}} = -8.7$  mag ( $2.4 \times 10^5 L_{\odot}$ ). The next brightest have  $M_{\text{bol}} = -8.2$  mag. These luminosity estimates are for stars without infrared excesses due to circumstellar shells. The  $H-K$  colors of the sample suggest that this is a good assumption. Core helium burning stars of initial mass 15–30  $M_{\odot}$  reach these luminosities after main-sequence lifetimes of  $\sim 10^7$  yr (Maeder 1981).

#### V. THE PERIOD-LUMINOSITY DIAGRAM

Figure 6 bears some resemblance to Figure 2 of WBF for the LMC. The  $P-L$  relation rises steeply from short periods, just as the AGB  $P-L$  relation does in the LMC, and then flattens at long periods, in a similar manner to the supergiant  $P-L$  relation in the LMC. But WBF noted a gap in luminosity between the tip of the AGB and the more luminous supergiant variables. This gap is shown graphically in Figure 7, in which their LMC data have been binned perpendicularly to their supergiant  $P-L$  relation:  $K = 9.36 - 0.0024 P$ . The period  $P$  is measured in days. The sampling parameter in this histogram is therefore  $x = \langle K \rangle + 0.0024 \times P$ , with a bin size of 0.1 mag. The data were smoothed with a Gaussian whose half width was 0.1 mag. The LMC distribution ranges between 8.5–12 mag, and is convincingly bimodal, the left-hand peak belonging to the supergiant LPVs and the right-hand peak belonging to the AGB LPVs.

<sup>1</sup> Replace the Cohen *et al.* (1981) sample with the smaller sample of Magellanic Cloud variable carbon stars of WBF, and one finds  $M_{\text{bol}} \approx -5.2$  mag. (This refers to the brightest three variable carbon stars in the SMC at  $[m-M]_0 = 18.7$ .) One should be cautious in comparing these small samples.

TABLE 2  
TIME-AVERAGED PHOTOMETRY

Star	P	$\langle J \rangle$	$\langle H \rangle$	$\langle K \rangle$	$m_{bol}$	n
	(day)	(mag)	(mag)	(mag)	(mag)	
P1322	458	16.77	15.86	15.54	18.57	3
P2426	770	14.83	14.09	13.74	16.63	2
P3482	539	15.51	14.83	14.56	17.19	3
P5900	203	17.91	16.68	16.29	19.38	3
P6283	760	14.19	13.54	13.31	15.79	2
P6836	1000	15.00	14.19	13.90	16.81	2
P7022	495	16.61	15.72	15.48	18.42	2
P9441	228	17.66	16.53	15.97	19.10	2
P11172	538	15.38	14.42	13.99	17.13	2
P11629	458	15.87	15.11	14.85	17.64	3
P11988	386	15.90	15.27	14.97	17.54	2
P14476	497	15.60	14.84	14.31	17.38	2
P16071	620	15.00	14.22	13.85	16.81	1
P16339	680	14.75	13.97	13.62	16.56	1
P18694	1200	14.70	14.03	13.44	16.49	2
P19844	700	15.54	14.88	14.49	17.33	2
P20917	760	14.72	13.97	13.60	16.53	1
P21091	685	14.84	14.09	13.66	16.65	2
P22330	950	15.17	14.25	13.78	16.93	2
P23152	386	17.63	16.83	16.00	19.09	3
P23182	589	15.06	14.27	13.97	16.86	2
P23324	398	16.07	15.24	15.18	17.67	2
P24355	600	14.92	14.12	13.76	16.73	2
P25017	980	14.54	13.78	13.46	16.35	2
P28639	478	14.96	14.13	13.77	16.77	2
P28986	497	14.65	13.97	13.64	16.41	2
P29476	680	15.05	14.28	13.92	16.87	2
P29926	1050	14.45	13.70	13.41	16.24	1
P32117	690	17.64	16.77	16.01	19.10	2
P32202	429	15.36	14.60	14.26	17.16	2
Q6508	600	14.82	14.09	13.81	16.57	3
Q6512	478	15.48	14.76	14.58	17.10	2
Q12254	815	14.72	13.94	13.52	16.52	2
Q14906	730	15.17	14.39	14.13	16.97	2
Q15476	231	17.52	16.73	16.67	19.08	2
Q16350	690	14.65	13.94	13.65	16.40	2
Q17032	650	15.17	14.41	14.18	16.90	2
Q17068	426	18.16	17.02	16.59	19.65	2
Q17675	760	14.85	14.06	13.74	16.66	2
Q18180	516	15.83	15.04	14.75	17.63	3
Q18569	770	16.23	15.32	15.01	18.03	2
Q21308	620	15.09	14.40	14.18	16.71	2
Q21736	516	15.72	14.94	14.63	17.52	2
Q21740	770	14.60	13.79	13.46	16.41	2
Q21765	458	15.86	15.03	14.72	17.67	1
Q22366	589	14.90	14.31	14.02	16.50	2
Q24798	346	15.68	14.99	14.78	17.28	2
Q29211	563	15.53	14.65	14.22	17.31	2
Q29250	429	16.21	15.68	15.33	17.81	2
Q29334	920	15.02	14.16	13.65	16.78	2
Q29631	539	15.58	14.79	14.41	17.39	2
Q31100	770	14.55	13.81	13.50	16.34	2
Q31267	589	14.77	14.05	13.82	16.45	2

Figure 7 also shows the corresponding distribution in M33 similarly constructed. The M33 distribution lies in the range  $14.5 < x < 18$  mag, but does not appear bimodal, although this could be a result of incompleteness. Although we have obtained complete photometry of the KMW sample, within that sample strong selection effects militate against finding faint, very red, large amplitude variables. We have successfully identified AGB variable stars in M33 (§ III), but their numbers may be much larger than the faint tail of Figure 7 would imply.

A first estimate of the distance modulus of M33 relative to the LMC can be obtained from the magnitude difference between the supergiant LPV peak in the LMC and the single peak in M33 in Figure 7. We can see the range of credible

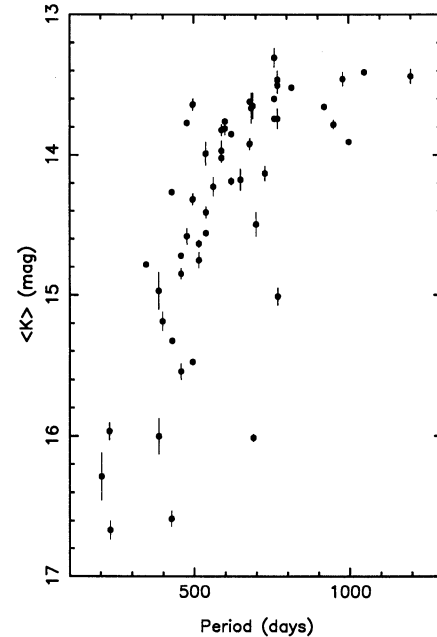


FIG. 6.—The period-luminosity relation from Table 2

relative distance moduli by fitting Gaussians with increasing half width to the peaks in Figure 7. The results are given in Table 3. The appropriate fit is a Gaussian with  $0.2 < \sigma < 0.4$ , implying  $\delta K = 6.2$  mag. A fit with  $\sigma = 0.1$  mag locks in on a narrow feature in the M33 distribution which could be due to noise.

This first estimate of the distance modulus difference ignores the fact the M33 peak in Figure 7 is broader than that of the LMC. Since the selection effects acting on the LMC sample are also hard to characterize, it is difficult to carry out any fair statistical tests to compare the LMC and M33 distributions. Formally, a  $\chi^2$  test indicates a probability less than 2% that either the LMC data ( $8.5 < x < 10$  mag) or the M33 data ( $14.8 < x < 16.3$  mag) are drawn from a common Gaussian distribution of  $\sigma = 0.23$  mag. Why is the supergiant LPV peak

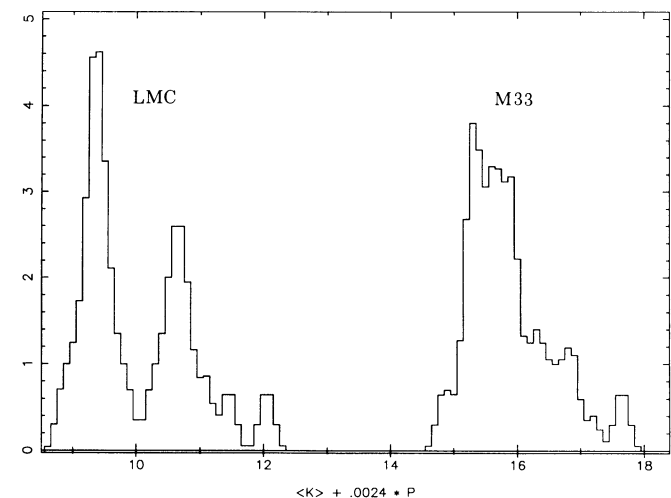


FIG. 7.—The distribution of stars in the  $P-L$  diagram. Stars are binned by  $x = \langle K \rangle + 0.0024 \times P$  rather than by  $\langle K \rangle$ . The distribution from  $x = 8-13$  mag is that of LMC LPVs from the work of Wood, Bessell, and Fox (1983). The distribution from  $x = 14-18$  mag is that of M33 LPVs from Table 2.



TABLE 3  
SEPARATION OF THE PEAKS IN  
FIGURE 7

$\sigma$	$x_{\text{LMC}}^{\text{pk}}$	$x_{\text{M33}}^{\text{pk}}$	$\delta x$
0.1.....	9.36	15.38	6.02
0.2.....	9.36	15.54	6.18
0.3.....	9.36	15.58	6.22
0.4.....	9.38	15.61	6.23
0.5.....	9.43	15.64	6.21

broadener in M33 than in the LMC? There are five possible effects that merit consideration:

1. *Reddening.* One needs a dispersion in the absorption  $A_K$  of  $\sim 0.3$  mag, which corresponds to a spread in  $E(J-H)$  of 0.33 mag. This can be ruled out from the two-color diagram in Figure 3. The spread in  $J-H$  for stars with  $K < 15.5$  is 0.08 mag rms.

2. *Metal Abundance Effects.* M33 shows a metal abundance gradient, unlike the LMC or SMC. Thus, if the  $P-L$  relation were abundance dependent, the gradient would smear out the peak in Figure 7. We examine this possibility further below.

3. *Slope of the  $P-L$  relation.* The value 0.0024 for the slope of the  $P-L$  relation is that obtained by KMW from the data of WBF, and is statistically uncertain by  $\pm 0.0002$ . The width of the M33 peak in Figure 7 is not reduced by changing the slope by twice this uncertainty.

4. *Period Errors.* KMW do not quote uncertainties in their measured periods, although they note that  $\sim 1000$  day periods are poorly determined. However, the slope of the supergiant  $P-L$  relation is so shallow that a 100 day error would be required to broaden the peak significantly in Figure 7, and this can be ruled out for a typical 500 day variable sampled over 1200 days. It seems probable that a small number of aliased periods are present on the KMW sample, but this should not be a dominant source of error.

5. *Confusion.* The small differences between imaging photometry in 1988 and single-channel photometry before that allow us to rule out photometric errors which are due to crowding as the origin of the broad  $P-L$  relation in M33.

Of these possible contributors to broadening the supergiant  $P-L$  relation, the range of chemical composition in M33 looks the most promising for closer examination. If we project all of the M33 LPVs on to the major axis of the Galaxy, using ellipses of the de Vaucouleurs, de Vaucouleurs, and Corwins' (1976) axial ratio, we see a weak correlation of  $x$  with radius, as shown in Figure 8. Assuming that all stars with  $x > 16.25$  are AGB stars, we obtain for the M33 supergiants  $x = 15.65 - 0.010 \times r$ , where  $r$  is the major axis radius in arc minutes. The slope coefficient is highly uncertain<sup>2</sup>:  $0.010 \pm 0.010$  mag arcmin<sup>-1</sup>.

The oxygen abundance gradient in M33 is documented in the review by Pagel and Edmunds (1981). The eight H II regions for which they report abundances show a strong linear correlation of  $\log(O/H)$  with radius. We obtain  $12 + \log(O/H) = 8.96 - 0.03 \times r$ , and transfer this to the upper horizontal scale in Figure 8. These correlations yield  $x = 15.45 \pm 0.14$  at the radius in M33 which corresponds in oxygen abundance to

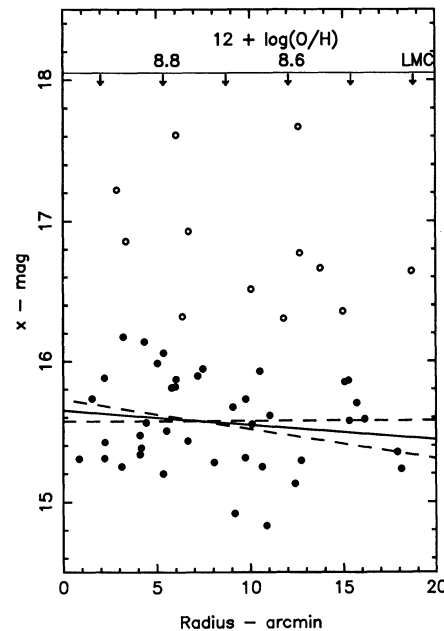


FIG. 8.—Variation with radius of  $x = \langle K \rangle + 0.0024 \times P$ . A linear fit to stars with  $x < 16.25$  mag (solid circles) is shown (solid line), together with the uncertainty in the regression (dashed lines). The oxygen abundance as a function of radius is indicated on the upper horizontal scale. An estimate of the relative distance modulus of M33 and the LMC can be obtained from the intersection of the solid line and the LMC abundance marker on this scale.

the LMC (Pagel and Edmunds 1981). This yields  $\delta x(\text{M33-LMC}) = 6.09 \pm 0.14$ . We adopt this improved estimate of  $\delta x$ , although (1) it is not significantly different from our first estimate, (2) the uncertainty is a good deal larger than if we ignore possible metallicity effects, and (3) a small extrapolation is involved.

Furthermore, it should be noted that metallicity variations do not seem to be the dominant broadening effect in Figure 7. The rms variation in  $\log(O/H)$  in M33 is  $\approx 0.13$ , this corresponds to  $\delta x \approx 0.05$  mag. The real source of the broad  $P-L$  relation in M33 remains for further investigation. In this sense, whether or not the correlation in Figure 8 is real, the corresponding  $\pm 0.14$  mag uncertainty in  $\delta x$  is a better indicator of the real uncertainty in the M33/LMC comparison than the small formal range in  $\delta x$  for  $\sigma \geq 0.2$  in Table 3. This uncertainty cannot be reduced until the excess width of the M33 peak in Figure 7 is understood.

Finally, it is appropriate to compare a relative distance modulus of  $\delta K = 6.09 \pm 0.14$  for supergiant LPVs with the corresponding estimate from RR Lyrae stars. The mean magnitude for seven RR Lyraes in the halo of M33 is  $\langle B \rangle = 25.79 \pm 0.15$  mag (Pritchet 1988). The mean magnitude for eight RR Lyraes in NGC 1786 in the LMC is  $\langle B \rangle = 19.57 \pm 0.05$  mag (Walker and Mack 1988). So  $\delta B = 6.22 \pm 0.16$  mag. The LPVs and RR Lyraes are therefore consistent provided that the reddening (and perhaps also the metallicity) of RR Lyraes in the two galaxies is not very different. According to the authors of these studies  $\delta A_B(\text{M33-LMC}) = -0.06 \pm 0.11$ . So  $\delta B_0 = 6.28 \pm 0.19$  mag. For Cepheids a number of estimates can be calculated from Feast's (1988) review. These are indicated in Table 4. With the exception of some larger values by Mould (1987), the Cepheid moduli suggest an *absolute* distance modulus  $\delta(m-M)_0 = 5.8$  mag, if the Population I reddening is as large as  $A_V = 0.3$ , as

<sup>2</sup> An upper limit on this slope coefficient close to the statistical one given here can be obtained by considering  $\delta x(\text{LMC-SMC})$ . This check is not as critical as one might hope, since only three of WBF's supergiant LPVs are in the SMC.

TABLE 4  
DIFFERENCE IN APPARENT DISTANCE MODULUS (M33-LMC)

Indicator	X bandpass	$\delta(m - M)_X$	Observations
LPVs .....	K	$6.09 \pm 0.14$	2
RR Lyraes .....	B	$6.22 \pm 0.15$	3
Cepheids .....	B	$6.14^1 \pm 0.11$	4
Cepheids .....	V	$6.01^1$	5
Cepheids .....	B	$6.11^1 \pm 0.05$	6
Cepheids .....	R	$6.25 \pm 0.03$	7
Cepheids .....	I	$6.32 \pm 0.11$	7
Cepheids .....	H	$5.86^1 \pm 0.11$	8

REFERENCES.—(1) Calculated from the review by Feast 1988; (2) this paper; (3) Pritchett 1988; (4) Sandage and Carlson; (5) Freedman 1985; (6) Christian and Schommer 1987; (7) Mould 1987; (8) Madore *et al.* 1985.

suggested by Feast. Additional multiwavelength observations of Cepheids in M33 would help to clarify the discrepancy between the long LPV modulus presented here, and the shorter modulus obtained from Cepheids.

## VI. CONCLUSIONS

The majority of the LPVs in the survey by KMW are supergiants. More than two-thirds of the sample is contained in the bolometric magnitude range  $-8.7$  mag, for the brightest star, to  $-7$  mag, the theoretical luminosity of the AGB tip. These stars are small amplitude variables (mean amplitude  $<0.05$  mag at K), and lightly reddened.

AGB stars are clearly present in the sample. They populate a period-luminosity relation with a distinctive slope, and one of them is a confirmed carbon star. However, the data do not make a convincing case for clear separation of the supergiant and AGB LPVs, as is seen in the LMC. The luminosity of the carbon star is  $M_{\text{bol}} = -5.3$  mag. This magnitude and that of

other carbon star candidates in the sample is consistent with the limiting luminosity observed for carbon stars in the Magellanic Clouds.

Comparison of the  $P-L$  relations for supergiant LPVs yields a distance modulus of  $\delta(m - M)_K = 6.09 \pm 0.14$  mag for M33 relative to the LMC. This is significantly larger than the value obtained at  $H$  for Cepheids by Madore *et al.* (1985). It is also significantly larger than the value which would be obtained from blue and visual observations of Cepheids, if they are reddened by a normal extinction law. It is possible that this discrepancy is due in part to higher circumstellar extinction affecting the M33 supergiant LPVs than affects LMC supergiant LPVs. However,  $A_K = 0.4$  mag corresponds to  $E(J - H) = 0.44$  mag and  $E(H - K) = 0.27$  mag, which is incompatible with Figure 2 and Figure 6 of Reid, Glass, and Catchpole (1988). A formal limit can be obtained by comparing  $\langle J - K \rangle$  for 37 stars with  $m_{\text{bol}} < 17.5$  mag in Table 2 with  $\langle J - K \rangle$  for 24 stars with  $M_{\text{bol}} < -7$  mag in the LMC sample of WBF. These values are  $1.10 \pm 0.02$  and  $1.12 \pm 0.02$  mag, respectively. We can conclude (with some allowance for possible systematic errors) that  $\delta\langle J - K \rangle(\text{M33-LMC}) < 0.05$ , and that  $\delta A_K < 0.028$  mag.

If we prefer Feast's (1988) estimates of the reddening of Population I in M33 ( $A_K = 0.03$ ) and the LMC ( $A_K = 0.008$ ), and assume a distance modulus of  $18.3 \pm 0.2$  mag for the LMC (Mould 1988) the new measurements reported here yield an absolute distance modulus  $\delta(m - M)_0 = 24.4 \pm 0.2$  mag from supergiant LPVs.

We gratefully acknowledge support for this project from NSF grant 85-02518 and 87-21705. We also thank Alain Picard for assistance in obtaining the carbon star spectrum, Vance Heron and Sean Lin for help with the infrared camera, and the staff of Palomar Observatory.

## REFERENCES

- Bessell, M., and Brett, J. 1988, *Pub. A.S.P.*, **100**, 1134.  
 Catchpole, R., Robertson, B., Evans, Lloyd, T., Feast, M., Glass, I., and Carter, B. 1981, *South African Astr. Obs. Circ.*, **1**, 61.  
 Christian, C. A., and Schommer, R. A. 1987, *A.J.*, **93**, 557.  
 Cohen, J., Frogel, J., Persson, S. E., and Elias, J. 1981, *Ap. J.*, **249**, 481.  
 de Vaucouleurs, G., de Vaucouleurs, A., and Corwin, H. 1976, *Second Reference Catalogue of Bright Galaxies* (Austin: University of Texas).  
 Elias, J., Frogel, J., and Humphreys, R. 1985, *Ap. J. Suppl.*, **57**, 91.  
 Elias, J., Frogel, J., Matthews, K., and Neugebauer, G. 1981, *A.J.*, **87**, 1029.  
 Feast, M. 1988, *Observatory*, **108**, 119.  
 Feast, M., Robertson, B., Catchpole, R., Evans, Lloyd, T., Glass, I., and Carter, B. 1982, *M.N.R.A.S.*, **201**, 439.  
 Freedman, W. 1985, in *IAU Colloquium 82, Cepheids: Theory and Observations*, ed. B. Madore (Cambridge: Cambridge University Press), p. 225.  
 Frogel, J., Persson, S. E., and Cohen, J. 1980, *Ap. J.*, **239**, 495.  
 Kinman, T. D., Mould, J. R., and Wood, P. R. 1987, *A.J.*, **93**, 833.  
 Madore, B., McAlary, R., McLaren, D., Welch, D., and Neugebauer, G. 1985, *Ap. J.*, **294**, 560.  
 Maeder, A. 1981, *Astr. Ap.*, **102**, 401.  
 Mould, J. 1987, *Pub. A.S.P.*, **99**, 1127.  
 ———, 1988, in *The Extragalactic Distance Scale*, ed. C. Pritchett and S. van den Bergh, (ASP Conf. Series **4**, 32).  
 Mould, J., and Aaronson, M. 1980, *Ap. J.*, **240**, 464.  
 Mould, J., Graham, J., Matthews, K., Soifer, B. T., and Phinney, E. S. 1989, *Ap. J. (Letters)*, **339**, L21.  
 Pagel, B., and Edmunds, M. 1981, *Ann. Rev. Astr. Ap.*, **19**, 77.  
 Pritchett, C. 1988, in *The Extragalactic Distance Scale*, ed. C. Pritchett and S. van den Bergh, (ASP Conf. Series, **4**, 59).  
 Reid, I. N., Glass, I., and Catchpole, R. 1988, *M.N.R.A.S.*, **232**, 53.  
 Sandage, A. R., and Carlson, G. 1983, *Ap. J. (Letters)*, **267**, L25.  
 van de Bergh, S., Herbst, E., and Kowal, C. T. 1975, *Ap. J. Suppl.*, **29**, 303.  
 Walker, A., and Mack, P. 1988, *A.J.*, **96**, 1362.  
 Wood, P. R., Bessell, M. S., and Fox, M. W. 1983, *Ap. J.*, **272**, 99.

JAY ELIAS: Cerro Tololo Inter-American Observatory, Casilla 603, La Serena, Chile 1353

JAMES R. GRAHAM and KEITH MATTHEWS: Caltech 320-47, Pasadena, CA 91125

JEREMY MOULD: Caltech 105-24, Pasadena, CA 91125

GERRY NEUGEBAUER: Caltech 103-33, Pasadena, CA 91125